

## Theoretical studies on the nature of bonding in $\sigma$ -hole complexes

A. Mohajeri\*, A.H. Pakiari, N. Bagheri

Department of Chemistry, College of Sciences, Shiraz University, Shiraz, Fars 71454, Iran

### ARTICLE INFO

#### Article history:

Received 12 August 2008

In final form 5 November 2008

Available online 11 November 2008

### ABSTRACT

Density functional investigation has been performed to explore structural and electronic properties of  $\sigma$ -hole bonded complexes formed from the interaction between  $\text{NH}_3$ ,  $\text{H}_2\text{O}$  and  $\text{HF}$  as nucleophile and molecules containing  $\sigma$ -hole atom of groups V–VII. It is found that the strength of interaction decreases in the order of  $\text{Cl} > \text{S} > \text{P}$  and  $\text{Br} > \text{Se} > \text{As}$ . This interaction is comparable or even stronger than the normal hydrogen bonding, however in the case where the nucleophile is not aligned in proper orientation with respect to the  $\sigma$ -hole atom the hydrogen bonding is preferred. The role of electrostatic potential in formation of  $\sigma$ -hole complex is also demonstrated and discussed.

© 2008 Elsevier B.V. All rights reserved.

### 1. Introduction

Theoretical study of hydrogen bonded systems and other weakly bonded complexes is a subject of great interest since they have significant effect on the structure of compounds in solid, liquid and gas phase and also affected the mechanisms of some processes. A specific type of noncovalent intermolecular interaction between a halogen atom in one molecule as electron acceptor and a negative site in another molecule as electron donor, is known as halogen bonding [1–5]. It has been known since the 19th century that dihalogens [6,7] and many organic halides [8] can form complexes with Lewis bases. These were sometimes described as ‘charge-transfer’ or ‘electron donor–acceptor’ interactions, and Mulliken [9] and later Flurry [10,11] developed theoretical formalisms for describing them.

More recently,  $\sigma$ -hole bonding has been identified by Politzer et al. [12,13] as an important noncovalent interaction, which is observed in divalently-bonded group VI atoms and trivalently-bonded ones of group V [12–22] as well as in covalently-bonded halides. Therefore, halogen bonding is simply a sub-category of  $\sigma$ -hole bonding. When the electron in a half-filled p orbital involves in forming a covalent bond, there follows a decrease in the electron density in another lobe of that p orbital. This electron-deficient outer lobe of half-filled p bonding orbital has been termed as ‘ $\sigma$ -hole’ [12,13]. If the electron deficiency is sufficient, a region of positive electrostatic potential is produced on the outer side of the atom, opposite to the covalent bond. Interaction of this type has been designed as  $\sigma$ -hole bonding and the molecule as  $\sigma$ -hole bond donor [20,21].

It is increasingly recognized that halogen bonding takes place in various biological systems and processes [1,23,24], and can be utilized effectively in drug design. Another area of application is crys-

tal engineering [25,26]; co-crystals can be produced that have specific desired features of structure and composition, leading to, for example, non-linear optical activity and enhanced conducting properties.

In the present work, a theoretical study has been performed on several complexes formed by  $\sigma$ -hole interaction between different molecules including phosphorous and arsenic in group V, sulfur and selenium in group VI and chlorine and bromine in group VII with  $\text{H}_2\text{O}$ ,  $\text{NH}_3$  or  $\text{HF}$  as nucleophile. The purpose of this effort is to explore the stationary geometries, interaction energies, and electronic properties of these  $\sigma$ -hole bonded complexes and in particular, to provide some valuable information of the nature and strength of  $\sigma$ -hole bonding.

### 2. Computational details

All calculations have been carried out with GAUSSIAN03 quantum chemistry [27] package in the electronic ground state using density functional theory (DFT) [28,29]. The geometries of all the monomers and dimers were fully optimized using B3PW91 with the 6-311++G\*\* basis set. The frequency calculations have been successfully performed to check all optimized ground state structures are in real minima. The interaction energy (IE) of each complex is calculated as the difference between the total energy of the complex and the sum of total energies of the nucleophile and the acceptor. The basis set superposition error (BSSE) is also taken into account by means of the Boys–Bernardi counterpoise (CP) technique [30].

Theory of atoms in molecules (AIM) [31] has been applied to characterize the  $\sigma$ -hole bonds in the investigated systems via AIM2000 package [32]. Also to provide more insights into the nature of this  $\sigma$ -hole bonding, natural bond orbital [33] (NBO) analysis was employed by the use of the natural bond orbital program implemented in the GAUSSIAN03 to characterize the bond in the investigated complexes. Natural population analysis (NPA) is also

\* Corresponding author. Fax: +98 711 2286008.

E-mail address: [amohajeri@shirazu.ac.ir](mailto:amohajeri@shirazu.ac.ir) (A. Mohajeri).

performed in the NBO framework. The charge-transfer energy ( $\Delta E_{CT}$ ) between donor and acceptor orbital have been obtained by second-order perturbation theory analysis of the Fock matrix. The interactions result in a loss of occupancy from the localized NBOs of the idealized Lewis structure into the empty non-Lewis orbital.

### 3. Results and discussion

The groups V–VII atoms that participate in  $\sigma$ -hole bonding usually have regions of both positive and negative electrostatic potential on their surfaces and thus can interact with both electrophile and nucleophiles. This was demonstrated in both experimental [34–36] and theoretical surveys [12,21,22]. In the present work, we study the  $\sigma$ -hole bonding arises from the interaction of positive electrostatic potentials, which are located on the extension of the covalent bonds to the groups V–VII atoms, with negative site on nucleophile. The  $\sigma$ -hole bonded complexes are presented by  $Z \cdots X-Y$  with three components: Z refers to nitrogen, oxygen or fluorine atom in the corresponding nucleophile  $NH_3$ ,  $H_2O$  or  $HF$ , X denotes an atom such as halogens, S, Se, P, or As, which contains  $\sigma$ -hole, and Y indicates an electron-withdrawing group such as  $-CN$  or electron donating group such as  $-OMe$ . The nature of the interactions has been analyzed by several points of view which are discussed below.

#### 3.1. Geometrical and energetic analysis

The calculated interaction energies for some  $\sigma$ -hole bonded complexes are given in Table 1. The basis set superposition errors (BSSE) have not been included since they all have small contribution (0.0004–0.0013 kcal/mol) to the total interaction energies.

It has been demonstrated that interaction energies of  $\sigma$ -hole bondings correlate with the magnitudes of surface electrostatic potential maxima on the atom containing  $\sigma$ -hole. The magnitude of the maximum positive electrostatic potentials,  $V_{s,max}$  reported by Politzer et al. [12] are given in Table 1 to compare its trend with our calculated interaction energies of the complexes under investigation.

The results in Table 1 show that as the  $V_{s,max}$  on  $\sigma$ -hole donor increases so does the strength of the interaction. Conversely,  $V_{s,max}$  can be predicted for X–Y compounds, if the trend of interaction energies of such  $\sigma$ -hole complexes is known. It is evident that the presence and magnitude of the positive electrostatic potential depends upon both the nature of X and the electron-withdrawing power of the Y group. For example, increasing the electron-withdrawing power of Y in the series of  $As(CH_3)_2-(OCH_3)$ ,  $As(CH_3)(CN)-(OCH_3)$ ,  $As(CN)_2-(OCH_3)$  and  $As(CN)_3$ , leads to more negative interaction energies. Therefore, electrostatic potential would offer a valuable tool for quantitatively understanding of various non-covalent interactions, such as hydrogen bonding and cation- $\pi$  interactions [37–40].

Our results demonstrate that the  $\sigma$ -hole bonding becomes stronger in going to down within groups V–VII as previously mentioned by Politzer et al. [1,12,21]. In addition, in a row the strength of interaction increases from left to the right. Thus, halogen of the lower row of the periodic table takes part in formation the strongest  $\sigma$ -hole interaction. Moreover, the interaction energy of  $\sigma$ -hole complex depends on the strength of nucleophile in such a way that it can be taken as a good criterion for strength of nucleophilicity of the nucleophile. The more strength of nucleophile, the more interaction energy can be expected for  $\sigma$ -hole bonded complex. For instance the interaction energies for  $H_3N \cdots ClCN$ ,  $H_2O \cdots ClCN$  and  $HF \cdots ClCN$  are  $-7.47$ ,  $-2.89$  and  $-1.32$  kcal/mol, respectively, suggesting the nucleophilicity trend as  $NH_3 > H_2O > HF$ , which is in agreement with experimental observations. It is found that  $NH_3$

**Table 1**

Some important geometrical parameters, interaction energies for  $\sigma$ -hole complexes and most positive electrostatic potentials of acceptors<sup>a</sup>.

Complex	IE	R	r	r'	$\angle ZXY$	$V_{s,max}$
1 $H_3N-ClCN$	-7.47	2.916	1.632	1.640	180	34.9 <sup>a</sup>
2 $H_3N-BrCN$	-9.66	2.822	1.787	1.809	180	42.1 <sup>a</sup>
3 $H_3N-SMeCN$	-6.78	4.085	1.689	1.690	168	30.8 <sup>d</sup>
4 $H_3N-SeMeCN$	-7.47	3.100	1.837	1.850	179	35.1 <sup>d</sup>
5 $H_3N-PMe_2CN$	-5.90	3.458	1.793	1.798	180	28.2 <sup>d</sup>
6 $H_3N-AsMe_2CN$	-6.27	3.273	1.925	1.938	178	30.2 <sup>d</sup>
7 $H_3N-ClOMe$	-8.16	2.587	1.721	1.752	178	19.1 <sup>d</sup>
8 $H_3N-BrOMe$	-11.47	2.558	1.864	1.898	178	26.6 <sup>d</sup>
9 $H_3N-SMeOMe$	-5.58	3.321	1.684	1.689	174	18.0 <sup>d</sup>
10 $H_3N-SeMeOMe$	-6.71	2.917	1.836	1.854	176	22.7 <sup>d</sup>
11 $H_3N-PMe_2OMe$	-	-	-	-	-	12.8 <sup>d</sup>
12 $H_3N-AsMe_2OMe$	-5.27	3.477	1.825	1.832	175	17.3 <sup>d</sup>
13 $H_3N-SMeF$	-8.28	2.624	1.667	1.706	176	28.8 <sup>b</sup>
14 $H_3N-SeMeF$	-12.05	2.517	1.809	1.861	179	34.8 <sup>b</sup>
15 $H_3N-PMe_2F$	-5.71	3.405	1.656	1.661	177	20.0 <sup>c</sup>
16 $H_3N-AsMe_2F$	-6.59	3.019	1.808	1.827	180	25.4 <sup>c</sup>
17 $H_3N-P(CN)_3$	-12.74	2.717	1.785	1.814	169	49.2 <sup>d</sup>
18 $H_3N-As(CN)_3$	-14.24	2.697	1.914	1.955	165	51.4 <sup>d</sup>
19 $H_3N-S(CN)_2$	-9.91	2.826	1.700	1.718	174	42.7 <sup>d</sup>
20 $H_3N-Se(CN)_2$	-12.11	2.769	1.846	1.878	171	46.9 <sup>d</sup>
21 $H_3N-PMe(CN)OMe$	-6.78	3.123	1.658	1.670	170	-
22 $H_3N-AsMe(CN)OMe$	-8.41	2.904	1.811	1.833	168	-
23 $H_2O-ClCN$	-2.89	2.897	1.632	1.634	180	34.9 <sup>a</sup>
24 $H_2O-BrCN$	-4.02	2.862	1.787	1.794	180	42.1 <sup>a</sup>
25 $H_2O-SMeCN$	-2.89	3.294	1.690	1.692	174	30.8 <sup>d</sup>
26 $H_2O-SeMeCN$	-3.51	3.104	1.837	1.845	174	35.1 <sup>d</sup>
27 $H_2O-PMe_2CN$	-2.57	3.272	1.793	1.796	179	28.2 <sup>d</sup>
28 $H_2O-AsMe_2CN$	-2.57	3.257	1.925	1.931	175	30.2 <sup>d</sup>
29 $H_2O-ClOMe$	-2.13	2.756	1.721	1.728	176	19.1 <sup>d</sup>
30 $H_2O-BrOMe$	-3.58	2.722	1.864	1.871	176	26.6 <sup>d</sup>
31 $H_2O-SMeOMe$	-	-	1.684	-	-	18.0 <sup>d</sup>
32 $H_2O-SeMeOMe$	-2.70	3.006	1.836	1.844	175	22.7 <sup>d</sup>
33 $H_2O-PMe_2OMe$	-	-	1.683	-	-	12.8 <sup>d</sup>
34 $H_2O-AsMe_2OMe$	-	-	1.825	-	-	17.3 <sup>d</sup>
35 $H_2O-SMeF$	-3.70	2.820	1.667	1.682	179	28.8 <sup>b</sup>
36 $H_2O-SeMeF$	-5.33	2.699	1.809	1.829	178	34.8 <sup>b</sup>
37 $H_2O-PMe_2F$	-	-	1.656	-	-	20.0 <sup>c</sup>
38 $H_2O-AsMe_2F$	-2.51	3.105	1.808	1.816	177	25.4 <sup>c</sup>
39 $HF-ClCN$	-1.32	3.092	1.632	1.632	179	34.9 <sup>a</sup>
40 $HF-BrCN$	-1.69	3.004	1.787	1.789	179	42.1 <sup>a</sup>

<sup>a</sup> Ref. [44].

<sup>b</sup> Ref. [21].

<sup>c</sup> Ref. [20].

<sup>d</sup> Ref. [12].

<sup>e</sup> R is  $\sigma$ -hole bonding distance, r and r' are bond lengths of X–Y before and after complexation (Å) and IE,  $V_{s,max}$  are in kcal/mol.

forms stronger  $\sigma$ -hole bonding with electron acceptors compared with  $H_2O$ , i.e. the higher electronegativity, the greater the attraction of lone pair. Therefore, oxygen with higher electronegativity will be less inclined to share its lone pairs with an acceptor. Also, in comparison between  $H_2O$  and  $HF$ , with the same reason  $HF$  forms weaker  $\sigma$ -hole bonding than  $H_2O$  and  $NH_3$ . In this direction, if we consider  $P(CH_3)_2F$ ,  $As(CH_3)_2-(OCH_3)$  and  $S(CH_3)-(OCH_3)$  with electrostatic potential 20.0, 17.3 and 18.0 kcal/mol, respectively, it is observed that they can form  $\sigma$ -hole complexes with  $NH_3$ , while the interaction cannot occur with  $H_2O$ . In the case, where the electrostatic potential is too weak,  $\sigma$ -hole interaction cannot be observed. For instance, in  $P(CH_3)_2-(OCH_3)$  in which the electrostatic potential is 12.8 kcal/mol we could not find  $\sigma$ -hole interaction either with  $NH_3$  or with  $H_2O$  and hydrogen bonding is preferred here.

There are also two important requirements, which should be satisfied for the  $\sigma$ -hole bonding formation; proper orientation and stereochemistry. When a nucleophile (as a Lewis base) becomes closer to a molecule containing  $\sigma$ -hole, the molecule must have proper stereochemistry (less steric effect) to form  $\sigma$ -hole bonding. For instance, in  $P(CH_3)_2-O(CH_3)$  the large steric effect of

methyl and methoxy groups on phosphorus prevents nucleophile to become closer along the extension of P–O and thus  $\sigma$ -hole bonding cannot be formed. Therefore, the hydrogen bonding between H<sub>2</sub>O and one hydrogen of a methyl group or between P and H<sub>2</sub>O are preferred. In addition, nucleophile such as nitrogen in NH<sub>3</sub> and oxygen in H<sub>2</sub>O, has at least one lone pair, which should be positioned in the opposite direction in line with the covalent bond between X and Y. In agreement to the previous report [12], our results demonstrate that the angles for Z··X–Y in the studied species are mostly near to 180°. The average deviation is about 6° and the largest nonlinearity is due to H<sub>3</sub>N··As(CN)<sub>3</sub> with 15° deviation from linearity. However, the highly directional nature of  $\sigma$ -hole interaction, which coincides with the positive centers on the atoms' surfaces, does indicate that it is electrostatically driven.

The selected optimized geometrical parameters such as bond distance for Z··X bond (*R*), X–Y distance before (*r*) and after complexation (*r'*) and ZXY angle are summarized in Table 1. The distances range from 2.5 to 3.5 Å in different complexes and they exhibit the opposite order of  $V_{s,max}$  within a group.

There are some hidden interactions that can compete or even interfere with  $\sigma$ -hole bonding such as hydrogen bonding [12]. In the complexes we studied here, two different cases have been observed; (a) if electrostatic potential is strong enough both  $\sigma$ -hole bonding and hydrogen bonding can be formed independently. There are one  $\sigma$ -hole bonding and one hydrogen bonding in H<sub>3</sub>N··S(CH<sub>3</sub>)–(OCH<sub>3</sub>) (Fig. 1a) and in H<sub>3</sub>N··As(CH<sub>3</sub>)<sub>2</sub>–(OCH<sub>3</sub>) we have one  $\sigma$ -hole and two hydrogen bondings (Fig. 1b). (b) In the case where  $V_{s,max}$  is very weak, hydrogen bonding is preferred (Fig. 1c). Therefore, electrostatic potential has essential role for making hydrogen bonding or multi hydrogen bonds parallel to  $\sigma$ -hole bonding.

### 3.2. Atoms in molecules and natural bond orbital

Bader's atoms in molecules theory has been successfully applied to study properties of a variety of conventional and unconventional hydrogen bonding and halogen bonding [41–43]. Accordingly, AIM calculations were carried out for  $\sigma$ -hole interactions in this work. Table 2 tabulates the electron density ( $\rho$ ), Laplacian ( $\nabla^2\rho$ ) and Hamiltonian energy (*H*) at the bond critical point of  $\sigma$ -hole bonding ( $\sigma$ -hole BCP) for these complexes.

A topological analysis of the electron density by AIM verifies the existence of  $\sigma$ -hole bonding between Z and X–Y in our complexes. Positive sign of both *H* and ( $\nabla^2\rho$ ) clearly indicates that  $\sigma$ -hole interactions are electrostatic dominant. Furthermore, the obtained values for electron density at BCP of  $\sigma$ -hole bonds are nearly in the range of normal hydrogen bonding. Moreover, the electron density at BCPs would be a convenient measure of  $\sigma$ -hole bond strength. It can be seen from Table 2 that the values of  $\rho$  are calculated to be in a range of 0.0065–0.0390 au and the electron density is increasing with increase of interaction energy. In the cases of H<sub>3</sub>N··Se(CH<sub>3</sub>)–OCH<sub>3</sub> and H<sub>3</sub>N··Se(CH<sub>3</sub>)–CN the interaction energy is larger for the latter while the electron density of N··Se is less. This indicates that the secondary interaction, hydrogen bonding, is taken place here which gives more stability to the second complex.

The interaction energy of  $\sigma$ -hole bond is almost comparable with the medium strength hydrogen bonding. The  $\sigma$ -hole interaction of NH<sub>3</sub> with Cl in H<sub>3</sub>N··ClCN gives –7.47 kcal/mol stability, while the hydrogen bond interaction in H<sub>3</sub>N··HCN makes the ammonia more stable (IE = –10.48 kcal/mol). In contrast, the interaction energy for  $\sigma$ -hole complex H<sub>3</sub>N··As(CN)<sub>3</sub> is –14.42 kcal/mol which is greater than the complex with hydrogen bond, H<sub>3</sub>N··HCN.

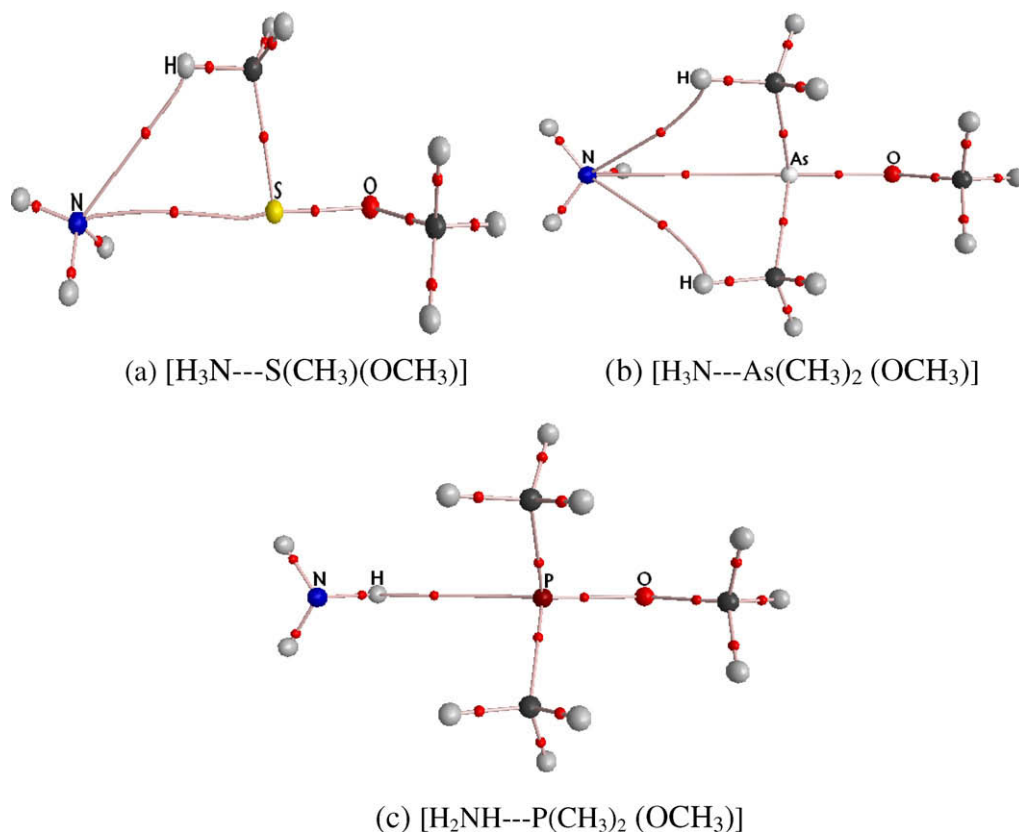


**Fig. 1.** Demonstration of  $\sigma$ -hole bonding and hydrogen bonding in some complexes: (a) one  $\sigma$ -hole bonding and one hydrogen bonding, (b) one  $\sigma$ -hole bonding along with two hydrogen bondings and (c) only hydrogen bonding.

**Table 2**

Computed electron density, Laplacian of electron density, Hamiltonian energy corresponding to the  $\sigma$ -hole bond critical points (a.u.), bond length variation ( $\text{\AA}$ ) and frequency shifts ( $\text{cm}^{-1}$ ).

Complex	$\rho$	$\nabla^2\rho$	$H$	$\Delta r$	$\Delta\omega$
1 H <sub>3</sub> N–ClCN	0.0154	0.0527	0.0216	0.008	–27.833
2 H <sub>3</sub> N–BrCN	0.0218	0.0644	0.0286	0.022	–40.893
3 H <sub>3</sub> N–SMeCN	0.0117	0.0332	0.0145	0.001	–1.770
4 H <sub>3</sub> N–SeMeCN	0.0093	0.0257	0.0097	0.013	–19.195
5 H <sub>3</sub> N–PMe <sub>2</sub> CN	0.0065	0.0183	0.0074	0.005	–7.899
6 H <sub>3</sub> N–AsMe <sub>2</sub> CN	0.0098	0.0244	0.0105	0.013	–14.999
7 H <sub>3</sub> N–ClOMe	0.0297	0.0920	0.0420	0.031	–57.449
8 H <sub>3</sub> N–BrOMe	0.0367	0.0972	0.0509	0.034	–35.826
9 H <sub>3</sub> N–SMeOMe	0.0067	0.0220	0.0086	0.005	–4.504
10 H <sub>3</sub> N–SeMeOMe	0.0182	0.0488	0.0223	0.018	–18.898
11 H <sub>3</sub> N–PMe <sub>2</sub> OMe	–	–	–	–	–
12 H <sub>3</sub> N–AsMe <sub>2</sub> OMe	0.0066	0.0180	0.0071	0.007	–4.048
13 H <sub>3</sub> N–SMeF	0.0286	0.0760	0.0370	0.039	–63.513
14 H <sub>3</sub> N–SeMeF	0.0390	0.0928	0.0542	0.052	–71.197
15 H <sub>3</sub> N–PMe <sub>2</sub> F	0.0072	0.0204	0.0081	0.005	–7.025
16 H <sub>3</sub> N–AsMe <sub>2</sub> F	0.0144	0.0416	0.0176	0.019	–14.752
17 H <sub>3</sub> N–P(CN) <sub>3</sub>	0.0264	0.0532	0.0290	0.029	–30.148
18 H <sub>3</sub> N–As(CN) <sub>3</sub>	0.0292	0.0616	0.0353	0.041	–48.005
19 H <sub>3</sub> N–S(CN) <sub>2</sub>	0.0206	0.0560	0.0259	0.018	–41.663
20 H <sub>3</sub> N–Se(CN) <sub>2</sub>	0.0254	0.0636	0.0319	0.032	–35.739
21 H <sub>3</sub> N–PMe(CN)OMe	0.0121	0.0292	0.0137	0.012	–10.933
22 H <sub>3</sub> N–AsMe(CN)OMe	0.0194	0.0448	0.0224	0.022	–23.378
23 H <sub>2</sub> O–ClCN	0.0117	0.0500	0.0196	0.002	–7.117
24 H <sub>2</sub> O–BrCN	0.0150	0.0576	0.0233	0.007	–29.323
25 H <sub>2</sub> O–SMe–CN	0.0066	0.0240	0.0096	0.002	–3.631
26 H <sub>2</sub> O–SeMeCN	0.0103	0.0343	0.0142	0.008	–11.191
27 H <sub>2</sub> O–PMe <sub>2</sub> CN	0.0065	0.0224	0.0091	0.003	–4.443
28 H <sub>2</sub> O–AsMe <sub>2</sub> CN	0.0070	0.0236	0.0094	0.006	–8.027
29 H <sub>2</sub> O–ClOMe	0.0172	0.0635	0.0268	0.007	–10.650
30 H <sub>2</sub> O–BrOMe	0.0215	0.0728	0.0322	0.007	–6.616
31 H <sub>2</sub> O–SMeOMe	–	–	–	–	–
32 H <sub>2</sub> O–SeMeOMe	0.0128	0.0392	0.0175	0.008	–8.062
33 H <sub>2</sub> O–PMe <sub>2</sub> OMe	–	–	–	–	–
34 H <sub>2</sub> O–AsMe <sub>2</sub> OMe	–	–	–	–	–
35 H <sub>2</sub> O–SMeF	0.0164	0.0502	0.0232	0.015	–16.907
36 H <sub>2</sub> O–SeMeF	0.0224	0.0691	0.0329	0.02	–19.25
37 H <sub>2</sub> O–PMe <sub>2</sub> F	–	–	–	–	–
38 H <sub>2</sub> O–AsMe <sub>2</sub> F	0.0101	0.0296	0.0130	0.008	–9.338
39 HF–ClCN	0.0056	0.0296	0.0106	0	–0.761
40 HF–BrCN	0.0086	0.0392	0.0151	0.002	–3.967

**Table 3**

NBO analysis of the  $\sigma$ -hole complexes<sup>a</sup>.

Complex	$q_z$	$q_x$	$q_y$	$\Delta E_{CT}$	$\chi$	$\gamma$
1 H <sub>3</sub> N–ClCN	–1.0596	0.1703	0.1494	3.42	1.23	0.021
2 H <sub>3</sub> N–BrCN	–1.0540	0.2281	0.0693	7.68	1.28	0.030
3 H <sub>3</sub> N–SMeCN	–1.0640	0.2860	0.0381	3.03	1.35	0.018
4 H <sub>3</sub> N–SeMeCN	–1.0615	0.4070	–0.0078	3.70	1.47	0.045
5 H <sub>3</sub> N–PMe <sub>2</sub> CN	–1.0645	0.7665	–0.0524	0.88	1.83	0.068
6 H <sub>3</sub> N–AsMe <sub>2</sub> CN	–1.0602	0.8502	–0.0611	2.82	1.91	0.084
7 H <sub>3</sub> N–ClOMe	–1.0138	0.1772	–0.5707	13.6	1.19	0.027
8 H <sub>3</sub> N–BrOMe	–1.0035	0.2339	–0.6455	22.00	1.24	0.036
9 H <sub>3</sub> N–SMeOMe	–1.0640	0.4586	–0.6839	0.69	1.52	0.044
10 H <sub>3</sub> N–SeMeOMe	–1.0482	0.5574	–0.7348	7.16	1.61	0.069
11 H <sub>3</sub> N–PMe <sub>2</sub> OMe	–	–	–	–	–	–
12 H <sub>3</sub> N–AsMe <sub>2</sub> OMe	–1.0624	1.1027	–0.8123	1.04	2.16	0.097
13 H <sub>3</sub> N–SMeF	–1.0347	0.5283	–0.5106	12.02	1.56	0.079
14 H <sub>3</sub> N–SeMeF	–1.0133	0.6045	–0.5803	25.30	1.62	0.097
15 H <sub>3</sub> N–PMe <sub>2</sub> F	–1.0669	1.0879	–0.5808	0.71	2.15	0.100
16 H <sub>3</sub> N–AsMe <sub>2</sub> F	–1.0552	1.1571	–1.0552	5.63	2.21	0.134
17 H <sub>3</sub> N–P(CN) <sub>3</sub>	–1.0474	0.8283	–0.0648	8.40	1.88	0.117
18 H <sub>3</sub> N–As(CN) <sub>3</sub>	–1.0433	0.9369	–0.0790	13.20	1.98	0.134
19 H <sub>3</sub> N–S(CN) <sub>2</sub>	–1.0574	0.4208	0.0412	5.30	1.48	0.056
20 H <sub>3</sub> N–Se(CN) <sub>2</sub>	–1.0498	0.5364	–0.0085	6.55	1.59	0.073
21 H <sub>3</sub> N–PMe(CN)OMe	–1.0598	1.0629	–0.8045	2.61	2.12	0.115
22 H <sub>3</sub> N–AsMe(CN)OMe	–1.0490	1.1303	–0.8154	7.77	2.18	0.141
23 H <sub>2</sub> O–ClCN	–0.9266	0.1772	0.1500	1.55	1.10	0.020
24 H <sub>2</sub> O–BrCN	–0.9285	0.2480	0.0701	3.24	1.18	0.028
25 H <sub>2</sub> O–SMe–CN	–0.9267	0.2958	0.0361	0.80	1.22	0.025
26 H <sub>2</sub> O–SeMe–CN	–0.9265	0.4062	–0.0079	2.41	1.33	0.039
27 H <sub>2</sub> O–PMe <sub>2</sub> CN	–0.9292	0.7539	–0.0511	0.63	1.68	0.065
28 H <sub>2</sub> O–AsMe <sub>2</sub> CN	–0.9279	0.8399	–0.0593	1.21	1.77	0.073
29 H <sub>2</sub> O–ClOMe	–0.9046	0.2001	–0.5487	4.49	1.10	0.024
30 H <sub>2</sub> O–BrOMe	–0.9016	0.2628	–0.6138	7.57	1.16	0.032
31 H <sub>2</sub> O–SMeOMe	–	–	–	–	–	–
32 H <sub>2</sub> O–SeMeOMe	–0.9172	0.5529	–0.7240	3.71	1.47	0.056
33 H <sub>2</sub> O–PMe <sub>2</sub> OMe	–	–	–	–	–	–
34 H <sub>2</sub> O–AsMe <sub>2</sub> OMe	–	–	–	–	–	–
35 H <sub>2</sub> O–SMeF	–0.9184	0.5410	–0.4869	4.24	1.46	0.062
36 H <sub>2</sub> O–SeMeF	–0.9109	0.6337	–0.5464	9.37	1.54	0.079
37 H <sub>2</sub> O–PMe <sub>2</sub> F	–	–	–	–	–	–
38 H <sub>2</sub> O–AsMe <sub>2</sub> F	–0.9253	1.1533	–0.6133	2.08	2.08	0.111
39 HF–ClCN	–0.5520	0.1711	0.1509	0.52	0.70	0.010
40 HF–BrCN	–0.5528	0.2443	0.0716	1.51	0.80	0.015

<sup>a</sup>  $\Delta E_{CT}$  is in kcal/mol.

A second order perturbation theory analysis of the Fock matrix was carried out to evaluate the donor–acceptor interaction in the NBO basis. In Table 3,  $\Delta E_{CT}$ ,  $q_x$ ,  $q_y$  and  $q_z$  for the  $\sigma$ -hole complexes are listed. The differences between the bond distances of X–Y ( $\Delta r = r' - r$ ) has been increased in all cases and has order of  $10^{-2}$  and  $10^{-3}$  as shown in Table 2. This lengthening of X–Y bond distance may be due to charge-transfer from lone pair of nucleophile to  $\sigma^*$  of X–Y, mainly  $n_z \rightarrow \sigma_{X-Y}^*$ , which is called hyperconjugation. The extent of total charge-transfer in this kind of complexes under our investigation is proportional to interaction energy and electrostatic potential shown in Table 3.

As can be seen in Table 3, there is correlation between interaction energy and difference of natural charge of atoms Z and X upon complex formation. The greater differences cause more stability in the formed complexes and led to stronger  $\sigma$ -hole bonding. Moreover it is observed that the interaction energies and charge-transfer  $\Delta E_{CT}$  are the same trend as  $\chi = |q_x - q_z|$ , and also  $\gamma = \frac{|q_z q_x|}{R_{ZX}^2}$  for couple of  $\sigma$ -hole complexes when Z and Y are fixed and X is different.

Table 2 demonstrates the decrease in frequencies of X–Y bond after formation of  $\sigma$ -hole complex,  $\Delta\omega = \omega_{X-Y(\text{complex})} - \omega_{X-Y(\text{fragment})}$ . The negative frequency change  $\Delta\omega < 0$  indicates the red shift which is due to increasing the X–Y bond length. Thus,  $\sigma$ -hole bonding in the complexes studied here can be classified as ‘normal bonding’ or ‘proper bonding’ while blue shift and bond

shortening are sometimes found to accompany  $\sigma$ -hole-bonding in some complexes [45,46].

#### 4. Conclusions

In the present study, interactions between NH<sub>3</sub>, H<sub>2</sub>O and HF as nucleophile and molecules containing  $\sigma$ -hole atom of groups V–VII have been theoretically investigated. Geometrical, energetic, AIM topological parameters and NBO analysis are our tools to study the nature of interactions. It was found that electrostatic potential  $V_{s,\text{max}}$  plays essential role in formation of  $\sigma$ -hole bond. Therefore, depending on the value of electrostatic potential one or multi hydrogen bonds can be formed parallel to  $\sigma$ -hole bonding. The highly directional nature of  $\sigma$ -hole bonding indicates that it is electrostatically dominant. Our results reveal that NH<sub>3</sub> acts as a stronger nucleophile than H<sub>2</sub>O and HF. The NBO analysis show that the X–Y covalent bond stretching is in correlation with the strength of  $\sigma$ -hole. According to the obtained results for the complexes studied here, charge-transfer interaction between lone pair on Z and X–Y  $\sigma^*$  orbitals leading to increase in the population of  $\sigma^*$  and elongate the X–Y bond.

#### References

- [1] P. Politzer, P. Lane, M.C. Concha, Y. Ma, J.S. Murray, J. Mol. Model. 13 (2007) 305.

- [2] A. Karpfen, E.S. Kryachko, Chem. Phys. Lett. 431 (2006) 428.
- [3] Q.C. Shi, Y.X. Lu, J.C. Fan, J.W. Zou, Y.H. Wang, J. Mol. Struct. (Theochem) 853 (2008) 29.
- [4] A. Ebrahimi, H. Roohi, S.M. Habibi, L. Behboodi, J. Mol. Struct. (Theochem) 712 (2004) 159.
- [5] M. Kubicki, J. Mol. Struct. 698 (2004) 67.
- [6] F. Guthrie, J. Chem. Soc. 16 (1863) 239.
- [7] I. Remsen, J.F. Norris, J. Am. Chem. 18 (1896) 90.
- [8] H.A. Bent, Chem. Rev. 68 (1968) 587.
- [9] R.S. Mulliken, J. Am. Chem. Soc. 74 (1952) 811.
- [10] R.L. Flurry Jr., J. Phys. Chem. 69 (1969) 1927.
- [11] R.L. Flurry Jr., J. Phys. Chem. 73 (1969) 2111.
- [12] P. Politzer, J. Murray, P. Lane, Int. J. Quantum Chem. 107 (2007) 3046.
- [13] T. Clark, M. Hennemann, J.S. Murray, P. Politzer, J. Mol. Model. 13 (2007) 291.
- [14] R.E. Rosenfield Jr., R. Parthasarathy, J.D. Dunitz, J. Am. Chem. Soc. 99 (1977) 4860.
- [15] T.N. Guru Row, R. Parthasarathy, J. Am. Chem. Soc. 103 (1981) 477.
- [16] J.P. Glusker, Top. Curr. Chem. 198 (1998) 1.
- [17] M. Iwaoka, H. Komatsu, T. Katsuda, S. Tomoda, J. Am. Chem. Soc. 124 (2002) 1902.
- [18] A.F. Cozzolino, I. Vargas-Baca, S. Mansour, A.H. Mahmoud-khani, J. Am. Chem. Soc. 127 (2005) 3184.
- [19] C. Bleiholder, D.B. Werz, H. Köppel, R. Gleiter, J. Am. Chem. Soc. 128 (2006) 2666.
- [20] J.S. Murray, P. Lane, P. Politzer, Int. J. Quantum Chem. 107 (2007) 2286.
- [21] J.S. Murray, P. Lane, T. Clark, P. Politzer, J. Mol. Model. 13 (2007) 1033.
- [22] P. Politzer, J.S. Murray, M.C. Concha, J. Mol. Model. 14 (2008) 659.
- [23] P. Auffinger, F.A. Hays, E. Westhof, H.P. Shing, Proc. Nat. Acad. Sci. 101 (2004) 16789.
- [24] P. Metrangolo, H. Neukirch, T. Pilati, G. Resnati, Acc. Chem. Res. 38 (2005) 386.
- [25] P. Metrangolo, G. Resnati, T. Pilati, Cryst. Eng. Comm. 8 (2006) 946.
- [26] F. Zordan, G.M. Espallargeas, L. Brammer, Cryst. Eng. Comm. 8 (2006) 425.
- [27] M.J. Frisch et al., Gaussian, Inc., Pittsburgh, PA, 2003.
- [28] J.W. Andzelm, in: J.K. Labanowski, J.W. Andzelm (Eds.), Density Functional Methods in Chemistry, Springer, New York, 1991, p. 155.
- [29] T. Ziegler, Chem. Rev. 91 (1991) 651.
- [30] S.F. Boys, F. Bernardi, Mol. Phys. 19 (1970) 553.
- [31] R.F.W. Bader, Atoms in Molecules: A Quantum Theory, Oxford University Press, Oxford, UK, 1990.
- [32] R.F.W. Bader, F. Biegler-König, J. Schönbohm, Am2000 Program Package, Ver. 2.0, University of Applied Sciences, Bielefeld, Germany, 2002.
- [33] A.E. Reed, L.A. Curtiss, F. Weinhold, Chem. Rev. 88 (1998) 899.
- [34] P. Murray-Rust, W.D.S. Motherwell, J. Am. Chem. Soc. 101 (1979) 4374.
- [35] P. Murray-Rust, W.C. Stallings, C.T. Monti, R.K. Preston, J.P. Glusker, J. Am. Chem. Soc. 105 (1983) 3206.
- [36] N. Ramasubbu, R. Parthasarathy, P. Murray-Rust, J. Am. Chem. Soc. 108 (1986) 4308.
- [37] V. Dimitrova, S. Ilieva, B. Galabov, J. Phys. Chem. A 106 (2002) 11081.
- [38] O. Lukin, J. Leszczynski, J. Phys. Chem. A 106 (2002) 6775.
- [39] L. Joubert, P.L.A. Popelier, Phys. Chem. Chem. Phys. 4 (2002) 4353.
- [40] S. Mecozzi, A.P. West Jr., D.A. Dougherty, J. Am. Chem. Soc. 118 (1996) 2307.
- [41] U. Koch, P.L.A. Popelier, J. Phys. Chem. 99 (1995) 9747.
- [42] P.L.A. Popelier, J. Phys. Chem. A 102 (1998) 1873.
- [43] S.J.J. Grabowski, Phys. Chem. A 104 (2000) 5551.
- [44] P. Politzer, J.S. Murray, M.C. Concha, J. Mol. Model. 13 (2007) 643.
- [45] P. Politzer, J.S. Murray, M.C. Concha, P. Lane, P. Hobza, J. Mol. Model. 14 (2008) 699.
- [46] W. Wang, N.B. Wong, W. Zheng, A. Tian, J. Phys. Chem. A 108 (2004) 1799.